

0
5
10
15
20
25
30
35
40
45

Authors Queries

Journal: **International Journal of Remote Sensing**

Paper: **246788**

Title: **Canopy blockage and scattering effects on apparent soil spectral reflectance and its consequence in spectral mixture analysis of vegetated surfaces**

Dear Author

During the preparation of your manuscript for publication, the questions listed below have arisen. Please attend to these matters and return this form with your proof. Many thanks for your assistance

Query Reference	Query	Remarks
1	Please supply reference for Duffie and Beckman (1991).	
2	Please define LAI.	
3	Please supply all author names for Jiang, Z. et al., 2006.	

0
5
10
15
20
25
30
35
40
45

Canopy blockage and scattering effects on apparent soil spectral reflectance and its consequence in spectral mixture analysis of vegetated surfaces

H. GUAN†, H. XIE*‡ and M. ZHU§

†School of Chemistry, Physics and Earth Sciences, Flinders University, South Australia, Australia

‡Department of Earth and Environmental Science, University of Texas at San Antonio, San Antonio, TX 78249, USA

§Research Center for GIS and RS, East China Institute of Technology, Fuzhou, Jiangxi 344000, China

(Received 26 November 2006; in the final form 16 March 2007)

The remote sensing technique has become the most efficient and common approach to estimate surface vegetation cover. Among various remote sensing algorithms, spectral mixture analysis (SMA) is the most common approach to obtain sub-pixel surface coverage. In the SMA, spectral endmembers (the number of endmembers may vary), with invariant spectral reflectance across the whole image, are needed to conduct the mixture procedure. Although the nonlinear effect in quantifying vegetation spectral reflectance was noticed and sometimes addressed in the SMA analysis, the nonlinear effect in soil spectral reflectance is seldom discussed in the literature. In this paper, we investigate the effects of vegetation canopy on the inter-canopy soil spectral reflectance via mathematical modelling and field measurements. We identify two mechanisms that lead to the difference between remotely sensed apparent soil spectral reflectance and actual soil spectral reflectance. One is a canopy blockage effect, leading to a reduced apparent soil spectral reflectance. The other is a canopy scattering effect, leading to an increased apparent soil spectral reflectance. Without correction, the first (second) mechanism causes an overestimated (underestimated) areal coverage of the low-spectral-reflectance endmember. The overall effect of canopy to soil, however, tends to overestimate fractional vegetation cover due to the relative significance of the canopy blockage effect, even two mechanisms varying as spectral wavelengths and the spectral difference between vegetation and soil. For SMA of vegetated surface using multiple-spectral remote sensing imagery (e.g., LandSat), it is recommended that infrared bands of low vegetation spectral reflectance (e.g. band 7) be first considered; if both visible and infrared bands are used, combination of bands 3, 4, and 5 is appropriate, while use of all six bands could overestimate fraction vegetation cover.

1. Introduction

Temporal and spatial distribution of surface vegetation coverage is of great concern in climatic, hydrologic, ecologic, forestry, and agricultural studies. Remote sensing

*Corresponding author. Email: hongjie.xie@utsa.edu

0 techniques are used to characterize surface vegetation cover because of their 0
efficiency, large spatial coverage and the availability of spatially and temporally
continuous data sets. Both multispectral (Smith *et al.*, 1990, DeFries *et al.*, 1999,
Elmore *et al.*, 2000, Small, 2001) and hyperspectral imagery (McGwire *et al.*, 2000,
5 Asner and Heidebrecht 2002, Williams and Hunt 2002) have been used to retrieve 5
surface areal vegetation coverage. Various algorithms, including those based on
vegetation index (Leprieur *et al.*, 2000, Lu *et al.*, 2003, Moreno Ruiz and Cantón
Garbin 2004, Jiang *et al.*, 2006) and those based on spectral reflectance (Smith *et al.*,
10 1990, Roberts *et al.*, 1993, Asner and Heidebrecht 2002, García-Haro *et al.*, 2005),
have been applied in the literature, although it is noticed that NDVI- and
reflectance-based models are not consistent in mathematics (Asner *et al.*, 2002). 10
Among these algorithms, the linear spectral mixture analysis (LSMA) is the most
accepted and applied approach to obtain sub-pixel fractional vegetation cover from
remote sensing imagery. The assumptions of LSMA are that the pixel spectral
15 reflectance retrieved from remote sensing imagery is the sum of spatially weighted
spectral reflectance of surface spectral endmembers, and that each endmember has
one specific and invariant spectral reflectance. However, due to the surface
(especially vegetation canopy) complexity, various types of nonlinear effects break
down (sometimes compromise) the LSMA assumptions. These nonlinear effects
20 include: (1) scale-dependent vegetation spectra induced by intra-canopy multi-
scattering (Williams, 1991), (2) shade (on canopy) and shadow (on inter-canopy soil)
(Gu and Gillespie 1998; Sabol Jr *et al.*, 2002; Berlow *et al.*, 2003), (3) radiometric
interactions between canopy and underlain soil (Ray and Murray 1996), and (4)
radiometric interactions between canopy and inter-canopy soil (Smith *et al.*, 1990;
25 Asner and Heidebrecht, 2002). Effects (1) and (3) are related to obtaining a remotely
sensed representative of the vegetation endmember, which can be achieved by
canopy-scale measurements or by appropriate mathematical analyses of the image
itself (Camacho-De Coca *et al.*, 2004). The shade and shadow problems (effect (2))
are often addressed by incorporating a shadow endmember into the LSMA model
30 (Fitzgerald *et al.*, 2005). However, the canopy effect on the inter-canopy soil spectral
reflectance (effect (4), other than the shadow) is rarely discussed in literature,
although the effect of soil spectra overshadowing the canopy is noticed (Asner and
Heidebrecht, 2002; Smith *et al.*, 1990), and soil effects on deriving vegetation indices
are reported (Huete and Tucker 1991; Bannari *et al.*, 1996).

35 In the LSMA model, each soil endmember reflectance viewed at a remote sensor is
assumed invariant and independent of other factors, such as fractional vegetation
cover and vegetation characteristics. Implicitly, it is assumed that the down-welling
irradiance over all inter-canopy soil surfaces is uniform. This assumption is
problematic because of the complexity of the canopy. Our hypothesis is that the
40 actual down-welling irradiance varies spatially due to two mechanisms: (1) the
canopy blocks (by reflecting and absorbing) some diffuse radiations from the sky
and (2) the canopy scatters some radiations to the nearby soil. The two mechanisms
may change the apparent soil spectral reflectance retrieved from the remote sensor in
different directions. The first mechanism (canopy blockage effect, hereafter) leads to
45 a reduced apparent spectral reflectance. This is more significant in visible bands
because a larger portion of diffuse radiation is in this spectral region. The second
mechanism (canopy scattering effect, hereafter) is more significant in the near-
infrared bands where the vegetation spectral reflectance is high. The objective of this
study is to test the hypothesis via mathematical modelling and field measurements,

and to examine the consequence of the canopy blockage and scattering effects on LSMA of surface fractional cover. The rest text is organized as follow: mathematical modelling of canopy effects on inter-canopy soil apparent reflectance and their consequent effects on LSMA (Section 2), field measurements used to test the mathematical modelling results (Section 3), the results of field tests (Section 4), and discussion and conclusions (Sections 5 and 6).

2. Mathematical modelling and experiments

2.1 Model development of Canopy effects on inter-canopy soil apparent reflectance

Quantitatively, the spectral reflectance is defined as the ratio of out-going spectral irradiance from a surface over in-coming (i.e., downwelling) spectral irradiance to the surface. The in-coming radiation includes direct radiation (or beam radiation) from the sun and diffuse radiation from the sky. Because the shorter wavelength range of solar radiation is easier to be scattered by the atmospheric constituents, the contribution of diffuse radiation in the total radiation is larger (figure 1).

Under ideal conditions (i.e. vegetation does not block or add radiation to its nearby soil), the down-welling spectral irradiance is

$$I' = B + D \quad (1)$$

where B is the beam radiation and D is the diffuse radiation from the clear sky. If, however, vegetation blocks diffuse radiation, or adds additional radiation by scattering to the soil (assuming vegetation is an isotropic reflector), the down-welling total short-wave irradiance is then

$$I = B + D[1 - f(x, h, w)] + (B + D)r_v f(x, h, w) \quad (2)$$

where x is the distance from the vertical projection of canopy edge on the ground, h

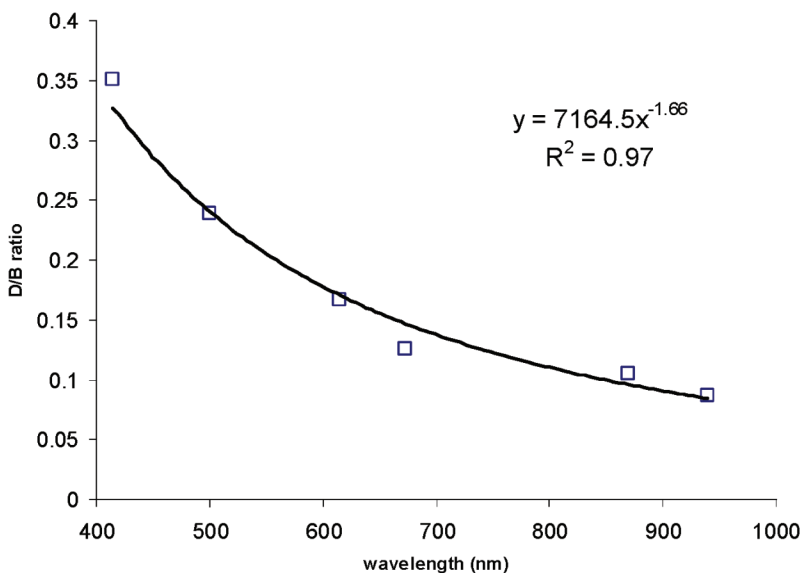


Figure 1. The ratio (δ) of diffuse radiation over beam radiation during ± 2 hours around noon derived from the measurements of May 24, 2005 (clear sky), at Point Reyes, California, USA (Data was downloaded from <http://www.archive.arm.gov>, June 2006).

is vegetation height, w is canopy width, r_v is the spectral reflectance of the canopy, and f is the function representing the portion of viewing hemisphere of the point at x blocked by the canopy (figure 2). The second term in the right-hand side of the equation represents the diffuse radiation to the inter-canopy soil, and the third term represents the additional radiation by canopy scattering. We assume that the canopy's view of the sky is not blocked. In other words, it scatters total downwelling radiation $r_v(B+D)$ uniformly to the hemisphere about the ground.

We approximately estimate f for one canopy situation using a simple geometric model. The canopy is assumed to have a cylindrical shape, with a diameter of w , and a height of h . The distance between the measurement point p and the leading edge of the canopy is x . Thus, the portion of sky viewed at point p blocked by the canopy is the ratio of canopy projection area on a hemisphere having a diameter of x over the area of the hemisphere above the ground. The area of hemisphere is $2\pi x^2$. The projection area of the canopy is approximated as a rectangle, with a width equal to the canopy diameter, and a length equal to the arc on the hemisphere with an angle of $a \tan (h/x)$. Because the width of canopy projected on the hemisphere cannot exceed the diameter of the hemisphere ($2x$), the width is equated to $2x$ when w is larger than $2x$.

$$f(x, h, w) = \frac{\min(w, 2x) x \operatorname{atan}(h/x)}{2\pi x^2} \quad (3)$$

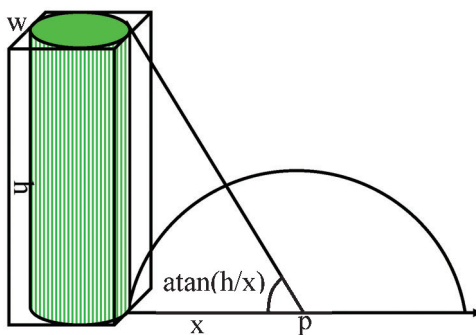
or

$$f(x, h, w) = \frac{\frac{\min(w, 2x)}{h} \operatorname{atan}(h/x)}{2\pi \frac{x}{h}} \quad (4)$$

In equation (4), when x approaches zero, $a \tan (h/x)$ is $\pi/2$, and f is equal to $1/2$, consistent with the situation that half of the sky is blocked by the canopy. When x is infinity, f is zero, indicating no canopy-blocked sky.

Substituting equation (4) into equation (2), we have

$$I = (1 + \delta)B + \left[-\delta B \frac{\frac{\min(w, 2x)}{h} \operatorname{atan}(h/x)}{2\pi \frac{x}{h}} \right] + (1 + \delta)B r_v \frac{\frac{\min(w, 2x)}{h} \operatorname{atan}(h/x)}{2\pi \frac{x}{h}} \quad (5)$$



COLOUR
FIGURE

Figure 2. Schematic of field of view at observation point p blocked by a hypothetical canopy, where h and w are the height and width of the canopy, respectively, and x is the distance to the edge of the canopy.

where δ is the ratio of D/B . With atmospheric and zenith angles (of solar and sensor) of corrected remote sensing data, the soil surface spectral reflectance should be

$$r = \frac{I_{out}}{I} \quad (6)$$

where I_{out} is the target radiation received at the remote sensor after atmospheric correction. If the vegetation blockage and scattering effects are not considered, the apparent spectral reflectance (e.g., viewed at the satellite remote sensor) is given by:

$$r' = \frac{I_{out}}{I'} \quad (7)$$

Thus,

$$r' = r \left[1 + \left\{ -\frac{\delta}{1+\delta} f(x, h, w) \right\} + r_v f(x, h, w) \right] \quad (8)$$

The second term of the numerator represents the vegetation blockage effect, which is a function of canopy aspect ratio (w/h), relative distance from the edge of the canopy and the ratio of diffuse over-beam radiation. The third term represents the vegetation scattering effect, which is a function of canopy aspect ratio, relative distance and the vegetation spectral reflectance. When we apply endmember reflectance for LSMA with satellite remote sensing data, we should use r' for the soil, which varies with distance to the canopy. However, r is often used instead of r' for LSMA. This simplification will cause LSMA estimating errors, the magnitude of which is dependent on the difference between r and r' .

To examine how significant the canopy blockage and scattering effects vary with distance, equation (8) is applied on a hypothetical surface with vegetation (2 m in height and 1 m in width) and soil spectral reflectance shown in figure 3. The results are presented in six bands equivalent to the six visible and near infrared bands of LandSat ETM+ imagery (figure 4). Consistent with our hypothesis, the apparent soil spectral reflectance decreases when approaching the canopy edge for the visible

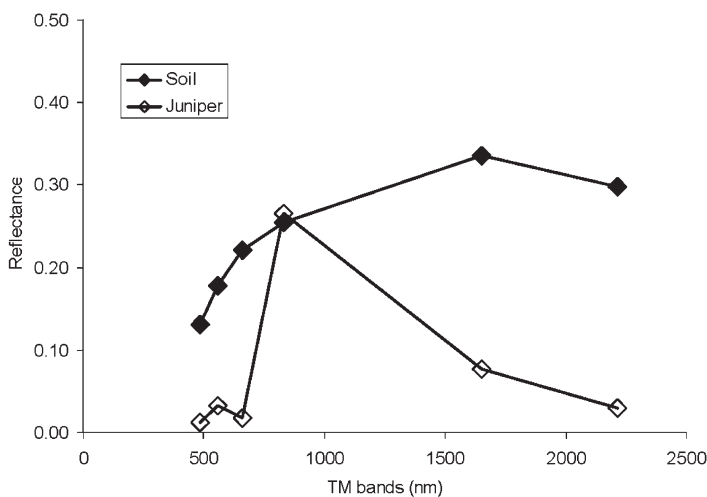


Figure 3. Field measured spectral reflectance of canopy-scale juniper and intercanopy soil, for the narrow-band regions equivalent to LandSat ETM+ bands.

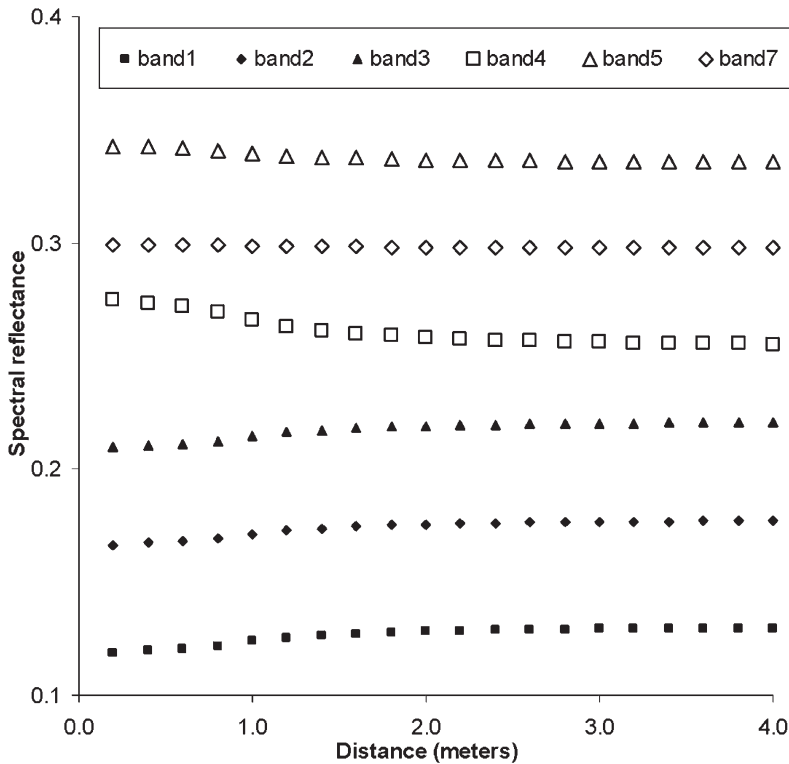


Figure 4. Modelled apparent soil spectral reflectance of six bands (equivalent to bands of LandSat ETM+) based on pure spectral reflectance shown in figure 3, with a hypothetical vegetation height of 2 m, and width of 1 m.

bands, and increases for the near infrared bands. Both canopy blockage and scattering effects decay to negligible at a distance of about the vegetation height. The effects are negligible for band 7.

2.2 Effect of canopy-modified soil apparent reflectance on LSMA

The effect of varying apparent soil reflectance on LSMA-estimated fraction vegetation cover is associated with the magnitude of all endmember spectral reflectance. With the example of vegetation and soil spectral reflectances shown in figure 3, for a single canopy of 2 m height, 1 m wide, the average change of apparent soil reflectance modified by nearby canopy is calculated based on equation (8) (figure 5). The relative significance of varying apparent soil reflectance impact is clearly observed at various bands, as well as at the three inter-canopy spacings. The reduced apparent soil reflectance in the visible bands is associated with the reduced down-welling irradiance to the soil surface due to the canopy-blockage effect. The LSMA with remote sensing imagery, which assumes invariant down-welling irradiance, overestimates the low-reflectance endmember (often vegetation). For the infrared bands, vegetation scattering effect is more important, leading to increased soil apparent reflectance, based on which the LSMA underestimates low-reflectance endmembers. If the overlapping effects of multiple canopies are considered (which were not included in figure 5), the impact will be much larger. For example, if it is assumed that the blockage and scattering effects of multiple

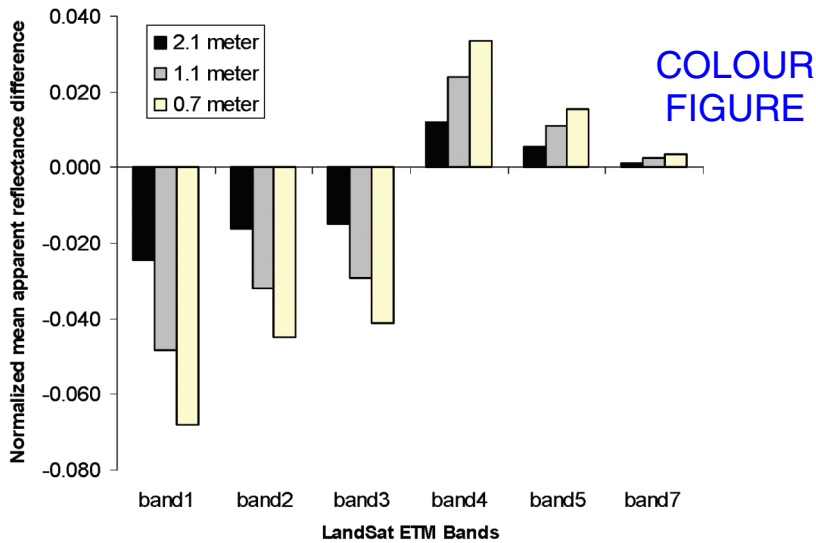


Figure 5. The mean difference between the apparent spectral reflectance of the soil surface due to one canopy within three selected distances from the canopy edge, normalized by the sum of vegetation and soil spectral reflectance. This number is equivalently proportional to the canopy blockage and scattering effects on LSMA derived fraction vegetation coverage. The calculation does not include the overlapping effects of multiple vegetation canopies, otherwise, the number would be several times larger.

canopies on intercanopy soil are about four times that caused by one canopy shown in figure 5, the LSMA of band 1 will overestimate fractional vegetation cover by about 10%, 20%, and 30% in absolute number for intercanopy spacing of one, one half, and one third of the vegetation height (i.e., if the actual vegetation cover is 25%, the estimation would be 35%, 45%, and 55%, respectively).

3. Field measurements

To test the mathematical experiments presented in the previous section, field measurements were conducted at two study sites. One was located on the campus of the University of Texas at San Antonio (UTSA), the other was located in Sevilleta National Wildlife Refuge (NWR) of New Mexico, the major study area of the Sevilleta Long-Term Ecological Research (LTER) programme (Hobbie *et al.*, 2003). For simplicity, the first site was referred to as the TX site, and the second as the NM site. The hyperspectral signatures were collected with a portable hyperspectral spectroradiometer (model FieldSpec©Pro FR, Analytical Spectral Devices, Inc., Boulder, CO). The spectroradiometer covers visible to mid-infrared wavelength regions (350–2500 nm), with a spectral resolution of about 3 nm in the visible and near-infrared portion of the spectrum (350–1050 nm) and 10–12 nm in the short-wavelength infrared portion of the spectrum (1050–2500 nm). The sampling interval is 1.4 nm for the 350–1050 nm region and 2 nm for the 1050–2500 nm region. Measurement was carried out under clear sky conditions, in the period of two hours around noon. The hyperspectral irradiance of white reference was collected at a location far away from the canopy (at least two times the vegetation height) for all measurements described below.

For the TX site, well-controlled canopy and intercanopy soil hyperspectral measurements were collected in October and November of 2005. The inter-canopy soil measurements were conducted by referring to two selected canopies. One was a juniper canopy, with a height of 2 m, and a diameter of 2 m. The other was a live oak canopy, with a height of 7 m, and a diameter of 8 m (figure 6). To avoid disturbance due to the spatial variability in spectral signature of inter-canopy space, a movable square metre of fine sand was placed on the ground to mimic a physically uniform soil surface. This movable sand was moved along a straight line outwards from the edge of canopy and spectral radiance measurements were carried out at each stop (every 20 cm). The sand was placed on site several hours before start of the measurements, and the sand surface was carefully smoothed to reduce anisotropic effects. The hyperspectral radiance of the sample sand surface was collected at two heights (30 cm and 100 cm) at each stop from the edge of canopy. To reduce temporal variation of the sky condition, for each distance (stop), white-reference radiance was collected separately, which was then used to calculate the soil spectral reflectance at that distance.

Measurements of canopy-scale and leaf-scale of a juniper were also conducted at the TX site. For the canopy-scale measurements, a lifter was used to locate the hyperspectral radiometers 4 m above the juniper canopy (2 m in both height and diameter). The results were averaged from three measurements. For the leaf-scale measurements, the sensor was placed a few centimeters above the targets of measurements. A few dozens of measurements were conducted and then averaged.

Measurements at the NM site were conducted in April and May of 2003. Two plots of juniper-dominant vegetated surfaces were selected along the eastern slope of Los Pinos Mountains, in central New Mexico. Each plot was of 710 m \times 430 m (or 25 \times 15 = 375 pixels of an ETM+ image). Both plots were within the coverage of one selected Landsat ETM+ image (path 33/row 36, acquired on June 16, 2002). The measurements were conducted before the rainy season of 2003, similar to the LandSat ETM+ image that was used in the study. The site was covered by piñon, juniper (dominant), dry grass (minor) and soil. The hyperspectra of the inter-canopy soils were collected at locations at least two times vegetation height away from the canopy edge. As indicated in figure 4, this measurement should give a soil reflectance very close to r in equation (8). It was difficult to obtain canopy-scale hyperspectra in the Los Pinos Mountains. So the canopy-scale spectral reflectance of the juniper collected in the TX site mentioned above was assumed to represent that of the NM



Figure 6. The two vegetation individuals: juniper (2 m height and 2 m diameter on the left), and oak (7 m height and 8 m diameter on the right) chosen for soil spectral reflectance measurements at the UT San Antonio main campus.

site. Although this approximation may introduce some uncertainty in the following data analysis, the error should be very small because leaves are the predominant component of the juniper canopies and the leaf-scale sunlit hyperspectral measurements of the juniper at the NM site were fairly similar to those at the TX site (not shown). To measure the fractional vegetation cover at the NM site, seven cells with the same size as an ETM+ pixel ($\sim 30\text{ m} \times 30\text{ m}$) were arbitrarily selected from the two plots. The maximum crown diameter of each individual tree within each cell was measured, and used to estimate crown area by vertical projection. The fractional vegetation cover of each cell was then calculated by summing crown areas and dividing by the cell area.

4. Results

Because of the contrast in complexity of actual measurement situations and simplification in mathematical modelling, the results of field measurements are qualitatively compared with mathematical results (i.e., the trend of spectral reflectance of inter-canopy soil varying with distance from the canopy is compared). The inter-canopy soil apparent reflectance measurements at the TX site are summarized in figures 7 and 8. There are some differences between the apparent reflectance collected at two heights (30 cm and 100 cm), but the trend of the spectral reflectance with distance is similar.

The canopy scattering effect is observed clearly for bands 4 and 5 for the juniper: reflectivity decreases as distance increase, while less clearly (but still observed) for the oak tree. This could be due to the difference in canopy structure, leaf area index, and leaf orientation between the two canopies. For example, the juniper leaves orient sub-vertically, which facilitates scattering to ground, while the oak leaves orient sub-horizontally, with dark sides facing the ground. The canopy blockage effect, reflectance increases as the distance increases, is obvious at bands 1

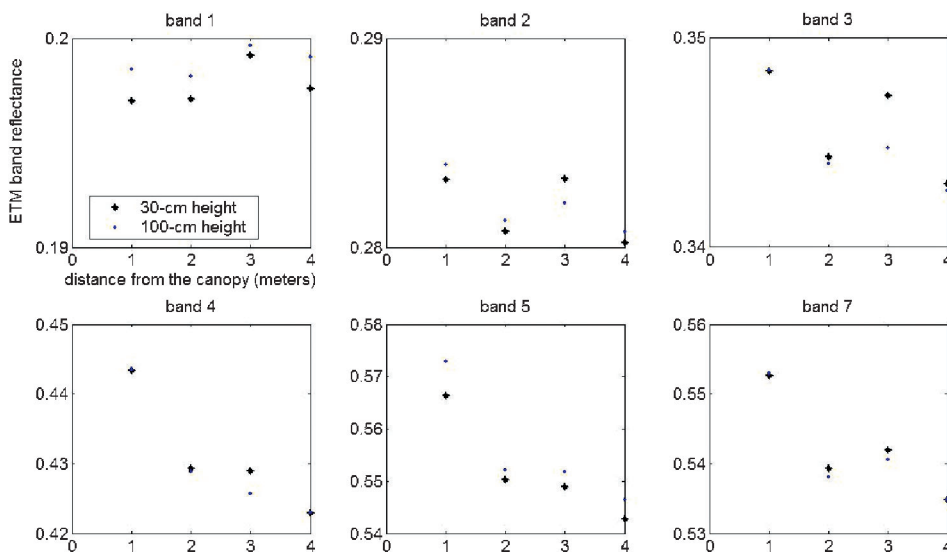


Figure 7. The apparent six ETM+ band reflectances of the sand sample as a function of distance to the southeast of the canopy edge (juniper, height of 2 m). Data was collected at times around noon ($>12:00$ local time) in November 2005 (TX site), with clear sky conditions.

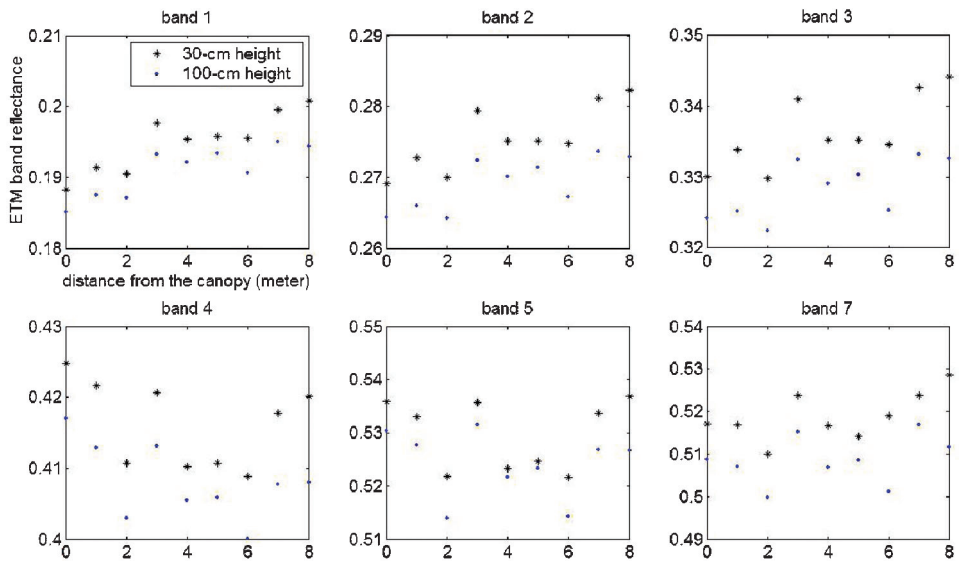


Figure 8. The apparent six ETM+ band reflectances of the sand sample as a function of distance to the west of the canopy edge (oak, height of 7 m). Data was collected at times around noon (>12:00 local time) in November 2005 (TX site), with clear sky conditions.

and 2 for the oak as expected, but not for the juniper. This is probably because (1) the blockage effect of the juniper is small due to its small canopy and (2) some tall dry grasses on the inter-canopy space scatter radiations and dampen the juniper blockage effect. The tall dry grasses near the juniper canopy may also account for the unexpected large band 7 reflectance. Given the simplified assumption in the mathematical model and complex situations of the actual surfaces, some inconsistencies between actual measurements (figures 7 and 8) and modelling results thus result as above. Overall, however, the canopy blockage effect is clearly supported by the measurements at the large-size oak canopy (blockage effect is dominant), and the canopy scattering effect is supported by the measurements at the juniper with dense leaves (scattering effect is dominant).

To examine how large the canopy blockage and scattering effects are on LSMA-estimated fractional vegetation cover, we applied the LSMA model (Appendix I) for each individual band and all available bands on the NM site. Since the spectral reflectance of dry grass (not shown) is close to that of the soil, and the dry grass cover is sparse at the NM site, only soil endmember was used for the inter-canopy space. In other words, we used soil hyperspectra and canopy-scale juniper hyperspectra (figure 3) as two endmembers to unmix the pixel spectra from Landsat image for estimating the fractional vegetation cover in each pixel.

The ETM+ image was corrected for atmospheric effect using a dark pixel subtraction approach (Chavez Jr, 1988) over the pixel radiance values (not DN values). The effect of solar zenith angle (24 degree) on down-welling radiation to the Lambertian surface was considered to derive pixel reflectance from radiance values. A digital elevation model (DEM) of 30 m \times 30 m resolution was applied to correct for the topographic effect using an algorithm developed by Duffie and Beckman (1991). With these corrections, we assume that the derived pixel reflectance represents the reflectance of the actual surface. Since canopy-scale juniper spectral

measurements were used, we assume that the error of fractional vegetation coverage estimation due to canopy endmember spectral uncertainty was negligible. Thus, any significant difference between LSMA-derived fractional vegetation cover and the field measurement is most likely due to using one-single soil reflectance r , instead of using varying reflectance r' .

The LSMA resulted fractional vegetation cover (Fr) with comparison to the field measurements is summarized in figure 9, in which the nine-pixel average (surrounding the field measured pixel) was used for the modelling result, to reduce the uncertainty due to co-registration error (using the center pixel also gave similar results, not shown). As predicted by the mathematical experiments shown in figure 5, the LSMA model strongly overestimates vegetation fraction using only band 1 (canopy blockage effect to soil), and slightly underestimates using band 5 (canopy scattering effect to soil), and gives fairly good estimates with band 7. With all six bands included, the LSMA model as expected strongly overestimates vegetation fraction when the contribution of each band is equally weighted for the sum of least squares error (i.e., the error divided by the pixel spectral reflectance). Specifically averaged for the seven arbitrary selected pixels, band 1 overestimates the fractional vegetation cover by 13% in absolute value (e.g., if the actual Fr=30%, LSMA of band 1 gives 43%), band 5 underestimates by 5%, the combination of all six bands with equal weights overestimates by 8%, and with varied weights (absolute square errors of individual bands) slightly overestimates by 3% on average for the seven measured pixels. The reason for the slight overestimate is that the infrared band is over-weighted in the sum of least squares error in the LSMA model due to the larger spectral reflectance than the visible bands.

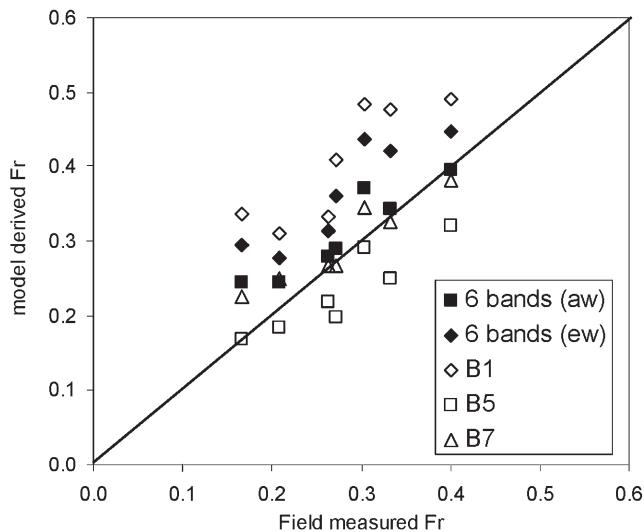


Figure 9. The LSMA derived pixel fractional vegetation covers vs. field measurements using least squares error criteria, based on all six Landsat ETM bands (solid symbols, aw=absolute square error for each band, ew=equal weight to calculate the sum of least squares error for all bands) and three selected individual bands (open symbols) for juniper-vegetated surfaces (with small portion of piñon) along the eastern slopes of Los Pinos Mountains, central New Mexico.

5. Discussion

The effect of varying apparent soil reflectance on LSMA estimated fraction vegetation cover is associated with the magnitude of endmember spectral reflectance. If the endmember spectral reflectance is smaller, a slight change of apparent reflectance has to be balanced by a significant change in fractional cover in LSMA modelling. For example, a change of apparent soil reflectance of 0.01 (absolute value) for all bands, on a simple two-end-member surface with an actual Fr of 0.3 (figure 3), will lead to an LSMA derived Fr change of 0.08 in absolute value (or about 30% relatively) for band 1. For vegetated surfaces, the spectral reflectance of visible bands is usually low; the canopy blockage effect could lead to significant overestimates of surface vegetation cover. The vegetation scattering effect on increased soil reflectance is most significant at near infrared bands (e.g., ETM band 4, MODIS band 2), which may lead to an underestimated fractional vegetation cover. For middle infrared (e.g., ETM band 7), both vegetation reflectance and sky diffuse components are small, thus the canopy blockage and scattering effects are small.

Because multiple bands are often used for LSMA modelling, the above-discussed effects may trade off to some degree. This probably explains why the canopy blockage and scattering effects on soil reflectance have not been documented and discussed in the literature. In terms of LSMA calculation based on multiple bands, the error due to the two investigated mechanisms is at a similar range due to other processes (e.g., nonlinear effects). Nonetheless, this error is predictable, and thus should be removed, so that other errors can be directly examined.

6. Conclusions

By mathematical modelling and field measurements, we examined the canopy blockage and scattering effects on apparent inter-canopy soil spectral reflectance, and their consequence in multispectral LSMA modelling of fractional vegetation cover. The canopy blockage effect is dominant in visible bands, and reduces apparent soil reflectance retrieved from remote sensors. Consequently, it leads to LSMA overestimates of fractional vegetation cover by an order of 10% in absolute fraction for the tested NM sites. The canopy scattering effect is dominant in infrared bands where the vegetation spectral reflectance is large. It often causes LSMA underestimation of fractional vegetation cover by a few percent in the absolute fraction, as demonstrated for the tested NM sites. These results suggest that canopy blockage and scattering effects are important phenomena, and should be seriously considered in spectral mixture analyses. It should be noted that the surface we examined here has relatively tall vegetation and high LAI. For surfaces with low-LAI and small 2 vegetation, canopy scattering and the blockage effect are not as significant. Instead, the reverse process, i.e., soil effect posed on the canopy spectra, can be significant.

For LSMA of vegetated surface with multiple bands, it is recommended that infrared bands of low vegetation spectral reflectance (e.g., LandSat band 7) be first considered. If both visible and infrared bands are used, careful selection of band combinations is suggested. For example, for the LandSat TM imagery, combination of bands 3, 4, and 5 is appropriate. Use of all six bands could overestimate fraction vegetation cover.

Acknowledgements

Valuable discussion with Xiaobing Zhou from Montana Tech is appreciated. Blake Weissling helped with some field work. This project was partially supported by a

0 TexasView Remote Sensing Consortium (a member of USGS/AmericanView Consortium) grant and a US Department of Education grant (P120A050061). The authors would like to thank two anonymous reviewers for their helpful comments that improved the paper.

5 References

- ASNER, G.P. and HEIDEBRECHT, K.B., 2002, Spectral unmixing of vegetation, soil and dry carbon cover in arid regions: Comparing multispectral and hyperspectral observations. *International Journal of Remote Sensing*, **23**, pp. 3939–3958.
- BANNARI, A., HUETE, A.R., MORIN, D. and ZAGOLSKI, F., 1996, Effects of soil color and brightness on vegetation indexes. *International Journal of Remote Sensing*, **17**, pp. 1885–1906.
- BERLOW, E.L., D'ANTONIO, C.M. and SWARTZ, H., 2003, Response of herbs to shrub removal across natural and experimental variation in soil moisture. *Ecological Applications*, **13**, pp. 1375–1387.
- CAMACHO-DE COCA F., GARCÍA-HARO, F.J., GILABERT, M.A. and MELIÁ, J., 2004, Vegetation cover seasonal changes assessment from TM imagery in a semi-arid landscape. *International Journal of Remote Sensing*, **25**, pp. 3451–3476.
- CHAVEZ JR, P.S., 1988, An improved dark-object subtraction technique for atmospheric scattering correction of multispectral data. *Remote Sensing of Environment*, **24**, pp. 459–479.
- DEFRIES, R.S., TOWNSHEND, J.R.G. and HANSEN, M.C., 1999, Continuous fields of vegetation characteristics at the global scale at 1-km resolution. *Journal of Geophysical Research D: Atmospheres*, **104**, pp. 16911–16923.
- ELMORE, A.J., LOBELL, D.B., MUSTARD, J.F. and MANNING, S.J., 2000, Quantifying vegetation change in semiarid environments: Precision and accuracy of spectral mixture analysis and the normalized difference vegetation index. *Remote Sensing of Environment*, **73**, pp. 87–102.
- FITZGERALD, G.J., CLARKE, T.R., PINTER JR, P.J. and HUNSAKER, D.J., 2005, Multiple shadow fractions in spectral mixture analysis of a cotton canopy. *Remote Sensing of Environment*, **97**, pp. 526–539.
- GARCÍA-HARO, F.J., SOMMER, S. and KEMPER, T., 2005, A new tool for variable multiple endmember spectral mixture analysis (VMESMA). *International Journal of Remote Sensing*, **26**, pp. 2135–2162.
- GU, D. and GILLESPIE, A., 1998, Topographic normalization of Landsat TM images of forest based on subpixel Sun-canopy-sensor geometry. *Remote Sensing of Environment*, **64**, pp. 166–175.
- HOBBIE, J.E., CARPENTER, S.R., GRIMM, N.B., GOSZ, J.R. and SEASTEDT, T.R., 2003, The US Long Term Ecological Research Program. *BioScience*, **53**, pp. 21–32.
- HUETE, A.R. and TUCKER, C.J., 1991, Investigation of Soil Influences in Avhrr Red and near-Infrared Vegetation Index Imagery. *International Journal of Remote Sensing*, **12**, pp. 1223–1242.
- JIANG, Z., *et al.*, 2006, Analysis of NDVI and scaled difference vegetation index retrievals of vegetation fraction. *Remote Sensing of Environment*, **101**, pp. 366–378. 3
- LEPRIEUR, C., KERR, Y.H., MASTORCHIO, S. and MEUNIER, J.C., 2000, Monitoring vegetation cover across semi-arid regions: Comparison of remote observations from various scales. *International Journal of Remote Sensing*, **21**, pp. 281–300.
- LU, H., RAUPACH, M.R., MCVICAR, T.R. and BARRETT, D.J., 2003, Decomposition of vegetation cover into woody and herbaceous components using AVHRR NDVI time series. *Remote Sensing of Environment*, **86**, pp. 1–8.
- MCGWIRE K., MINOR, T. and FENSTERMAKER, L., 2000, Hyperspectral mixture modeling for quantifying sparse vegetation cover in arid environments. *Remote Sensing of Environment*, **72**, pp. 360–374.

- 0 MORENO RUIZ, J.A. and CANTÓN GARBÍN, M., 2004, Estimating burned area for tropical Africa for the year 1990 with the NOAA-NASA pathfinder AVHRR 8 km land dataset. *International Journal of Remote Sensing*, **25**, pp. 3389–3410.
- 5 RAY, T.W. and MURRAY, B.C., 1996, Nonlinear spectral mixing in desert vegetation. *Remote Sensing of Environment*, **55**, pp. 59–64.
- 10 ROBERTS, D.A., SMITH, M.O. and ADAMS, J.B., 1993, Green vegetation, nonphotosynthetic vegetation, and soils in AVIRIS data. *Remote Sensing of Environment*, **44**, pp. 255–269.
- 15 SABOL JR, D.E., SMITH, M.O., TUCKER, C.J., GILLESPIE, A.R. and ADAMS, J.B., 2002, Structural stage in Pacific Northwest forests estimated using simple mixing models of multispectral images. *Remote Sensing of Environment*, **80**, pp. 1–16.
- 20 SMALL, C., 2001, Estimation of urban vegetation abundance by spectral mixture analysis. *International Journal of Remote Sensing*, **22**, pp. 1305–1334.
- SMITH, M.O., USTIN, S.L., ADAMS, J.B. and GILLESPIE, A.R., 1990, Vegetation in deserts: I. A regional measure of abundance from multispectral images. *Remote Sensing of Environment*, **31**, pp. 1–26.
- WILLIAMS, A.P. and HUNT JR, E.R., 2002, Estimation of leafy spurge cover from hyperspectral imagery using mixture tuned matched filtering. *Remote Sensing of Environment*, **82**, pp. 446–456.
- WILLIAMS, D.L., 1991, A comparison of spectral reflectance properties at the needle, branch, and canopy level for selected conifer species. *Remote Sensing of Environment*, **35**, pp. 79–93.

Appendix I

The linear spectral mixture analysis model is a common method used to obtain fractional vegetation cover within a pixel from the remote sensing imagery. It is defined as

$$\sum_j (R_{ij} X_j) = R_i \quad (A1)$$

with the constraint equation

$$\sum_j X_j = 1 \quad (A2)$$

where R_{ij} is the reflectance of the j th endmember for band i , X_j is the fractional surface area covered by the j th end-member, and R_i is the remotely sensed reflectance of the pixel at band i .

For a two-endmember surface, at least one band is needed to solve the unknown X_j (or Fr in the text), given the endmember reflectance and the pixel reflectance. If multiple bands are used, we have more than two equations to solve two unknowns (i.e., soil and vegetation fractional cover). In this situation, we use a least squares error algorithm to solve equations for fractional vegetation cover. Based on how the squared error of each band is weighted into the sum of error from all bands, we can have two different algorithms. We can either equally weigh the error of each band, or weigh the error of a band using the relative importance of pixel reflectance of that band.